

Effective Sublattice Magnetization and Néel Temperature in Quantum Antiferromagnets

Eduardo C. Marino and Marcello B. Silva Neto
Instituto de Física, Universidade Federal do Rio de Janeiro,
Caixa Postal 68528, Rio de Janeiro - RJ, 21945-970, Brazil
 (March 9, 2018)

We present an analytic expression for the finite temperature effective sublattice magnetization which would be detected by inelastic neutron scattering experiments performed on a two-dimensional square-lattice quantum Heisenberg antiferromagnet with short range Néel order. Our expression, which has no adjustable parameters, is able to reproduce both the qualitative behaviour of the phase diagram $M(T) \times T$ and the experimental values of the Néel temperature T_N for either doped $\text{YBa}_2\text{Cu}_3\text{O}_{6.15}$ and stoichiometric La_2CuO_4 compounds. Finally, we remark that by incorporating frustration and 3D effects as perturbations is sufficient to explain the deviation of the experimental data from our theoretical curves.

PACS numbers: 74.72.-h, 74.25.Ha, 74.72.Bk

Two dimensional quantum antiferromagnetism has been a matter of great interest and subject to intense investigation, due to its possible relation to the normal state properties of high-temperature superconductors. There is by now clear experimental evidence that the pure high- T_c superconducting cuprate compounds are well described by a quasi two-dimensional $S = 1/2$ Heisenberg antiferromagnet on a quasi-square lattice, whose sites are occupied by Cu^{++} magnetic ions. The dynamical structure factor of the 2D Heisenberg antiferromagnet, calculated via the mapping of the Heisenberg Hamiltonian onto the $O(3)$ nonlinear sigma model [1], was successfully confirmed by inelastic neutron scattering experiments on La_2CuO_4 [2]. Several other microscopic techniques like light scattering [3], muon spin relaxation [4] and thermal neutron scattering [5], have also been used to probe the magnetic correlations in these materials and confirmed the quasi 2D Heisenberg antiferromagnet hypothesis.

A common feature among almost all superconducting cuprate compounds is the existence of a Néel ordered moment in the low temperature, underdoped regime. As the temperature is increased, or the sample doped, antiferromagnetic order is destroyed, leading to new forms of spin order [6]. According to spin-wave theory, for a d-dimensional hypercubic lattice, Néel order is possible at $T = 0$ for $d \geq 2$. However, despite the widespread success of spin-wave theory, there remain a number of issues that defy the description of the superconducting cuprate compounds within this approach. For example, the development of a sublattice magnetization is known to be suppressed in the two-dimensional Heisenberg antiferromagnet for any nonzero temperature. True long range order, as a genuine three-dimensional phenomenon, would only be achieved by considering the interlayer coupling $J_\perp \sim 10^{-5} J_\parallel$ not only as a perturbation.

It is the purpose of this work to show that the experimental data for the sublattice magnetization of La_2CuO_4 [7] and $\text{YBa}_2\text{Cu}_3\text{O}_{6.15}$ [8] can in fact be described still in the context of a two-dimensional square-lattice quantum Heisenberg antiferromagnet at finite temperatures, as far as inelastic neutron scattering experiments are concerned. Our starting point is the observation that the nature of the spin correlations in the renormalized classical regime is consistent with one of the three possibilities of fig. 1, according to the observation wave vector $|k|$, or frequency ω [9]. In this sense, any possible neutron scattering experiment, with high enough energy transfers, performed on a true two-dimensional system, would actually measure a nonvanishing effective sublattice magnetization, since one would be probing the dynamics of spin correlations in the intermediate Goldstone region. Inelastic neutron scattering experiments probe a microscopic, short wavelength physics to which we can associate an effective Néel moment. As it will become clear, the behaviour of this effective moment can be described by an effective field theory for the low frequency, long wavelength fluctuations of the spin fields about a state with short range Néel order. We will then be able to speak about a finite temperature phase transition in the 2D system, associated to the collapse of the Goldstone region in fig. 1.

RENORMALIZED CLASSICAL

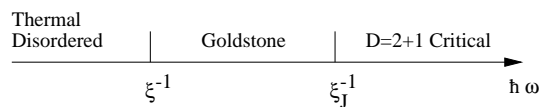


FIG. 1. Properties of the 2D quantum Heisenberg antiferromagnet as a function of the frequency ω . ξ is the actual correlation length while ξ_J is the Josephson correlation length related to the spin-stiffness by $\xi_J = \hbar c / \rho_s$.

The two-dimensional square-lattice quantum Heisenberg antiferromagnet has a well known continuum limit given in terms of the $2 + 1$ dimensional $O(3)$ quantum nonlinear sigma model [10]. The later, on the other hand, is defined by the partition function

$$\mathcal{Z}(\beta) = \int \mathcal{D}n_l \delta(n_l^2 - 1) \exp(-\mathcal{I}(n_l)), \quad (1)$$

where the action

$$\mathcal{I}(n_l) = \frac{\rho_0}{2\hbar} \int_0^{\beta\hbar} d\tau \int d^2\mathbf{x} \left[(\nabla n_l)^2 + \frac{1}{c_0^2} (\partial_\tau n_l)^2 \right] \quad (2)$$

describes the long-wavelength fluctuations of the staggered components of the spin-field $n_l = (\sigma, \vec{\pi})$, $l = 1, \dots, N = 3$. The fixed length constraint is understood. In the above expression, ρ_0 is the spin stiffness, c_0 is the spin-wave velocity, $\beta = (k_B T)^{-1}$ and all quantities with a 0 subscript represent bare quantities.

We shall work in the natural units $k_B = \hbar = c = 1$, with c being the renormalized spin wave velocity. * Also, further analysis will be simply expressed in terms of the coupling constant $g_0 = N/\rho_0$, which has the units of inverse length. With this notation and choosing the staggered magnetization to be along the σ field direction, we can integrate over the remaining $N - 1$ spin-wave degrees of freedom $\vec{\pi}$ and study the behavior of the partition function (1) in the large N limit. As usual, N is taken to be large enough while g_0 is kept fixed. This means that we have to choose $\rho_0 \sim N$.

For large N , the partition function (1) is dominated by the stationary configurations of the magnetization, $\langle \sigma \rangle$, and of the Lagrange multiplier field, $i\langle \lambda \rangle = m^2$, introduced in order to ensure the averaged fixed length constraint. These, on the other hand, can be determined from the stationarity conditions

$$m^2 \langle \sigma \rangle = 0, \quad \langle \sigma \rangle^2 = \frac{1}{g_0} - \frac{1}{\beta} \sum_{n=-\infty}^{\infty} \int_0^\Lambda \frac{d^2\mathbf{k}}{(2\pi)^2} \frac{1}{\mathbf{k}^2 + \omega_n^2 + m^2}, \quad (3)$$

where a cutoff Λ was introduced to make the momentum integral ultraviolet finite.

From the above set of equations we see that the antiferromagnetic system could in principle be found in two distinct phases. If $\langle \sigma \rangle \neq 0$ then $m = 0$ and the system would be in the Goldstone phase with a nonvanishing net sublattice magnetization. In this case the ground state would exhibit true long range Néel order. If $m \neq 0$ on the other hand, then $\langle \sigma \rangle = 0$ and Néel order is absent. There are no gapless excitations in the spectrum of the

finite temperature system. It is a well known fact that for the $2 + 1$ dimensional $O(N)$ invariant nonlinear σ model at $T > 0$, the only possible physical situation is the second one, due to severe infrared divergencies in the second saddle-point equation (3). As a consequence, the value of m is pushed from zero to a finite value making the sublattice magnetization $\langle \sigma \rangle$ to vanish, in agreement with the Coleman-Mermin-Wagner theorem.

We can compute the value of the $O(N)$ invariant mass m in a closed form by subtracting the linear divergence in the second saddle-point equation (3) as

$$\frac{1}{g_0} = \frac{1}{g_c} + \frac{\rho_s}{4\pi N}, \quad (4)$$

where $g_c = 4\pi/\Lambda$ is the bulk critical coupling and

$$\rho_s = \frac{\sqrt{S(S+1)} \hbar c}{2\sqrt{2} a}, \quad (5)$$

with $S = 1/2$ and a being the lattice spacing [10]. Now, after momentum integration and frequency sum we arrive at

$$\xi^{-1} = m(\beta) = \frac{2}{\beta} \operatorname{arcsinh} \left(\frac{e^{-\beta \rho_s / (2N)}}{2} \right), \quad (6)$$

which is nonvanishing for $T > 0$, thus indicating that a Néel phase can only occur at $T = 0$. The conclusion is that even at the smallest temperature there is a gap in the spin-wave spectrum and a finite correlation length which measures the size of clusters in which there is short range Néel order. The above expression for ξ has been obtained by Chakravarty *et al.* [1] and its zero temperature limit successfully confirmed by quasi-elastic neutron scattering experiments on La_2CuO_4 [11], for, however, temperatures approaching T_N from above, $T \rightarrow T_N^+$, where this compound is known to exhibit a true two-dimensional behaviour.

Let us now consider inelastic neutron scattering experiments, performed on a true $2D$ system, with energy transfers $\Delta E = \hbar\omega$ such that the corresponding wavelength, $\lambda = 1/\hbar\omega$, satisfies $\xi_J \leq \lambda \leq \xi$. Typical time scales in such experiments are $\tau_\lambda = \lambda/c$, consequently much smaller than the relaxation time $\tau = \xi/c$ at which the $2D$ system disorders. For such experiments, spins would look like as if they were frozen and a nonvanishing effective sublattice magnetization would be measured. Since at low temperatures ξ is much larger than ξ_J , the three regions of fig. 1 are well separated. In the large intermediate region, probed by our experiment, the system behaves as if it had true long range antiferromagnetic order and dynamic scaling hypothesis is justified [1]. We are then allowed to apply a hydrodynamic picture for the low frequency, long-wavelength fluctuations of the spin-fields n_l , in which its short-wavelength fluctuations follow adiabatically the fluctuations of the disordered background

*For large N the spin wave velocity does not renormalize and $c_0 = c$.

whose typical wavelenth is the scale of disorder, the correlation length. The effective field theory to describe the spin correlations in this intermediate Goldstone region is obtained by functionally integrating the Fourier components of the fields in (1) with frequency inside momentum shells $\kappa \leq |\mathbf{k}| \leq \Lambda$. The resulting partition function is such that, for large N , the leading contribution now comes from the scale dependent stationary configurations $\langle \sigma \rangle_\kappa$ and $i\langle \lambda \rangle_\kappa = m_\kappa^2$, solutions of the new set of saddle-point equations

$$m_\kappa^2 \langle \sigma \rangle_\kappa = 0, \quad \langle \sigma \rangle_\kappa^2 = \frac{1}{g_0} - \frac{1}{\beta} \sum_{n=-\infty}^{\infty} \int_{\kappa}^{\Lambda} \frac{d^2 \mathbf{k}}{(2\pi)^2} \frac{1}{\mathbf{k}^2 + \omega_n^2 + m_\kappa^2}. \quad (7)$$

Differently from the previous case, now we can in fact find the system in two different phases (regimes): ordered (asymptotically free) or disordered (strongly coupled); depending on the size of $\xi_\kappa = 1/\kappa$ relative to ξ : smaller (high energies) or larger (low energies). In the ordered phase, $\xi_\kappa \ll \xi$, $m_\kappa = 0$ is the solution that minimizes the free energy and the $2D$ system is then characterized by a nonvanishing effective sublattice magnetization $\langle \sigma \rangle_\kappa \neq 0$, a divergent effective correlation length $\xi_{eff} = 1/m_\kappa = \infty$ and gapless excitations in the spectrum.

The effective sublattice magnetization can be exactly computed from the second saddle point equation (7). Using the renormalization scheme defined by (4), we obtain, after momentum integration and frequency sum, the expression

$$\frac{\rho_s(\kappa, \beta)}{2\pi N} \equiv \langle \sigma \rangle_\kappa^2 = \frac{\rho_s}{4\pi N} + \frac{1}{2\pi\beta} \ln(2 \sinh(\beta\kappa/2)), \quad (8)$$

which depends on the energy scale κ and on the temperature.

Some comments are in order. The running spin stiffness (8) decreases ($g(\kappa, \beta) = N/\rho_s(\kappa, \beta)$ increases) as $\xi_\kappa \rightarrow \xi$, for a given temperature. This is a consequence of the fact that we are coarsing over degrees of freedom which actually feels the finite size of the clusters with short range Néel order. Furthermore, for $\xi_\kappa > \xi$ we would be coarsing over degrees of freedom outside these clusters, leading to the disordered (strongly coupled) phase. Lowering the scale κ is also equivalent to waiting longer for a response, and for $\tau_\kappa \geq \tau$ we would be waiting long enough for the system to disorder. Here, conversely, in order to obtain a finite temperature phase transition in the $2D$ system, we will rather fix the scale κ and study the behaviour of the effective spin stiffness (8) with the running parameter being the temperature. We must fine tune, and hold fixed, the energy transfers in our experiment so that our $2D$ system is able to reproduce the observed $3D$ behaviour in real materials. For this it suffices to impose the boundary condition

$$\rho_s(\kappa, T = 0) = \rho_s, \quad (9)$$

with ρ_s being the bulk spin stiffness of the real system. From (9) we conclude that $\kappa = \rho_s/N$, which is exactly the inverse Josephson correlation length, $\kappa = \xi_J^{-1}$. This should not be surprising since the spin stiffness is itself a microscopic, short wavelength quantity defined at the Josephson scale. Notice also that $\kappa = 23$ meV for the case of La_2CuO_4 , which is actually consistent with the energy transfers commonly used in this kind of experiment [2]. Now, inserting (9) in (8), the expression for the finite temperature effective sublattice magnetization, $M(T) \equiv \rho_s(\kappa = \rho_s/N, T)$, becomes

$$M(T) = \frac{M_0}{2} + NT \ln \left(2 \sinh \left(\frac{M_0}{2NT} \right) \right), \quad (10)$$

with $M_0 = \rho_s$. The sublattice magnetization $M(T)$ vanishes at a Néel temperature T_N given by

$$T_N = \frac{M_0}{N \ln 2}. \quad (11)$$

For temperatures above T_N , we would be coarsing over degrees of freedom outside the shrunk clusters of size ξ , leading again to the disordered (strongly coupled) phase.

Let us now show that the above analysis can in fact be used to describe the experimental data for different cuprate compounds. Take for example the data obtained for La_2CuO_4 [7] and $\text{YBa}_2\text{Cu}_3\text{O}_{6.15}$ [8]. For these compounds, we find agreement between our predictions and the observed Néel temperatures, within almost 10%, already at the leading order, as can be seen from table I. More important, we have obtained a good qualitative agreement between the phase diagram $M(T) \times T$ and experiment, for the whole range of temperatures from 0 to T_N (see dotted lines in figs. 2 and 3).

In order to have a flavor on how our results can be improved, let us mention that already at the next-to-leading order in the $1/N$ expansion we will have a non-trivial renormalization of the spin-wave velocity due to the self interaction between spin-waves [9]. This should lower the value of c and, if we take for example a lowering of about 10%, we obtain the behaviour described by the solid curves in figs. 2 and 3. The spin wave velocity will also be renormalized by dynamic scaling, but we assume that at the shortest distances, that is $\hbar\omega \gg \xi^{-1}$, this effect can be neglected when compared to the effects of the self interactions. For this reason, it should not lead to a further damping of the spin waves.

	c (eV $\text{\AA}/\hbar$)	ρ_s (meV)	T_N (K)	T_N^{exp} (K)
YBa ₂ Cu ₃ O _{6.15}	1.00 ± 0.05	81 ± 4	450 ± 20	410 ± 3
	0.90 ± 0.05	73 ± 4	410 ± 20	
La ₂ CuO ₄	0.85 ± 0.03	68 ± 2	380 ± 10	325 ± 5
	0.75 ± 0.03	60 ± 2	330 ± 10	

TABLE I. To compute ρ_s we have made use of formula (5) with $a \sim 3.8$ \AA and $S = 1/2$, while to compute T_N we have used formula (11) with $N = 3$. The experimental values of c were taken from ref. [12].

Notice now that, with respect to the solid curves, the experimental points can be separated into two different sets. For $T < T_N/2$, we find all points below the solid curves while, for $T > T_N/2$, we find, instead, the points all above our theoretical prediction. This is consistent with a picture in which strong frustration induced quantum fluctuations, due for example to a nonzero next-nearest-neighbour coupling, are dominant at low temperatures and suppressed at higher T , where the effects due to a sizable J_\perp begin to be felt. Notice also that in the case of $\text{YBa}_2\text{Cu}_3\text{O}_{6.15}$ the points deviate even more from the solid curve, for $T > T_N/2$, than in the case of La_2CuO_4 . We attribute this to the bilayer structure of $\text{YBa}_2\text{Cu}_3\text{O}_{6.15}$, which causes a further increase in the sublattice magnetization. As we approach T_N from below, both systems behave effectively as true $2D$ Heisenberg antiferromagnets with nearest-neighbour coupling, as shown by the experimental data. From the above discussion we conclude that by incorporating frustration and $3D$ effects as perturbations, with properly temperature renormalized coefficients, might be sufficient to account for the deviation of the data from our theoretical predictions. We are presently investigating this possibility.

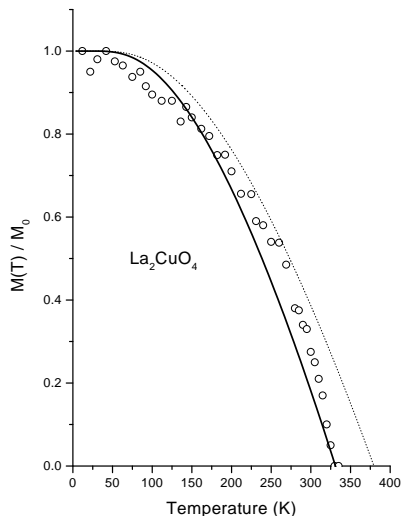


FIG. 2. For the dotted line we have used $\hbar c = 0.85$ eV \AA while for the solid line we assumed $\hbar c = 0.75$ eV \AA . Experimental data from ref. [7].

As a final remark, let us show that our treatment is consistent with experiment also in the disordered phase. Above T_N , where the effective sublattice magnetization vanishes, we must consider the second possible solution for the set of saddle-point equations (7), namely $\langle \sigma \rangle_\kappa = 0$ and $m_\kappa \neq 0$. If we then solve the self-consistent equation

for the gap we end up with

$$m_\kappa^2 = \frac{4}{\beta^2} \text{arcsinh}^2 \left(\frac{e^{-\beta \rho_s / (2N)}}{2} \right) - \left(\frac{\rho_s}{N} \right)^2, \quad (12)$$

for $\kappa = \rho_s / N$. It is straightforward to see that the effective correlation length $\xi_{eff} = 1/m_\kappa$ diverges as $T \rightarrow \rho_s / (N \ln 2)$, or in other words, as we approach T_N from above. This is consistent with the data for La_2CuO_4 from [11], and for the correct temperature limit.

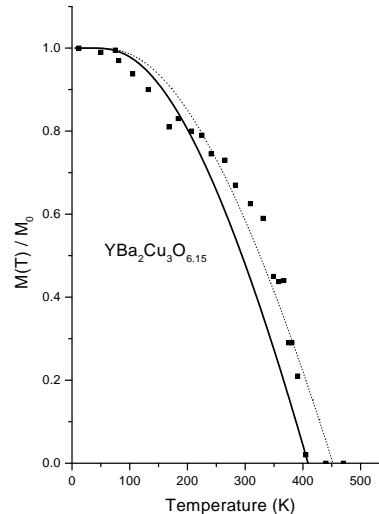


FIG. 3. For the dotted line we have used $\hbar c = 1.00$ eV \AA while for the solid line we assumed $\hbar c = 0.90$ eV \AA . Experimental data from ref. [8].

The authors have benefited from several fruitful discussions with C. Farina, A. Katanin, B. Keimer, E. Miranda and F. Nogueira. E.C.M. is partially supported by CNPq and FAPERJ. M.B.S.N is supported by FAPERJ.

-
- [1] S. Chakravarty *et al.*, Phys. Rev. **B39**, 2344 (1989).
 - [2] K. Yamada *et al.*, Phys. Rev. **B40**, 4557 (1989).
 - [3] K. Lyons *et al.*, Phys. Rev. **B37**, 2353 (1988).
 - [4] D. Harshman *et al.*, Phys. Rev. **B38**, 852 (1988).
 - [5] D. Vaknin *et al.*, Phys. Rev. Lett. **58**, 2802 (1987).
 - [6] E. C. Marino, Phys. Lett. **A263**, 446 (1999).
 - [7] B. Keimer *et al.*, Phys. Rev. **B45**, 7430 (1992).
 - [8] J. M. Tranquada *et al.*, Phys. Rev. Lett. **60**, 156 (1988).
 - [9] A. V. Chubukov *et al.*, Phys. Rev. **B49**, 11919 (1994).
 - [10] F. D. M. Haldane, Phys. Rev. Lett. **50**, 1153 (1983).
 - [11] Y. Endoh *et al.*, Phys. Rev. **B37**, 7443 (1988).
 - [12] A. P. Kampf, Phys. Rep. **249**, 219 (1994).